

Article

Occupancy prediction using low-cost and low-resolution heat sensors for smart offices

Beril Sirmacek and Maria Riveiro

Jönköping AI Lab (JAIL), Department of Computer Science and Informatics, School of Engineering, Jönköping University, Sweden

Email: beril.sirmacek@ju.se, maria.riveiro@ju.se

1 **Abstract:** In order to design efficient and sustainable office spaces and to automate lighting, heating
2 and air circulation in these facilities, solving the challenge of occupancy prediction is crucial. In office
3 spaces where large areas need to be observed, multiple sensors must be used for full coverage. In
4 these cases, it is normally important to keep the costs low, but also to make sure that the privacy of
5 the people who use such environments are preserved. Low-cost and low-resolution heat (thermal)
6 sensors can be very useful to build solutions that address these concerns. However, they are extremely
7 sensitive to noise artifacts which might be caused by heat prints of the people who left the space
8 or by other objects which are either using electricity or exposed to sunlight. There are some earlier
9 solutions for occupancy prediction that employ low-resolution heat sensors, however, they have not
10 addressed nor compensate for such heat artifacts. Therefore, in this paper, we present a low-cost
11 and low-energy consuming smart space implementation to predict the number of people in the
12 environment based on whether their activity is static or dynamic in time. We use a low-resolution
13 (8×8) and non-intrusive heat sensor to collect data from an actual meeting room. We propose two
14 novel workflows to predict the occupancy; one based on computer vision and one based on machine
15 learning. Besides comparing the advantages and disadvantages of these different workflows, we use
16 several state-of-the-art explainability methods in order to provide a detailed analysis of the algorithm
17 parameters and how the image properties influence the resulting performance. Furthermore, we
18 analyze noise resources which affect the heat sensor data. We hope that our analysis brings light
19 into understanding how to handle very low-resolution heat images in these environments. The
20 presented workflows could be used in various domains and applications other than smart offices,
21 where occupancy prediction is essential, e.g., for elderly care.

22 **Keywords:** heat sensors; smart offices; occupancy prediction; machine learning; computer vision;
23 feature engineering; explainability

24 1. Introduction

25 Designing smart environments have gained significant attention over the last years due to
26 advancements in sensor technology, decreased hardware cost (even edge devices) and ease of
27 deployment (using sensor fusion, cloud and Internet of Things –IoT– technologies). Using sensor
28 technologies combined with small and efficient hardware and intelligent algorithms, we are now able
29 to provide smart solutions that support humans at home and work, e.g., in business offices, school
30 buildings, hospitals, elderly facilities and wellness centers. Smart environments differ from traditional
31 environments because of real-time interactions between the users and the facilities; one important
32 research topic within this area is occupancy prediction and human activity detection/recognition, due
33 to their broad application in automation, robotics and human computer interaction (HCI).

34 Detecting human activities accurately and in real-time is a challenging problem for several reasons
35 [1]. There are several methods developed for the purpose of detecting human activity indoors, e.g.,
36 using multimedia-sources (such as audio/video), wearable devices (smartwatches, wristbands, etc.),
37 and ambient sensing. Each method comes with its advantages and disadvantages based on its use
38 cases. For instance, despite having high accuracy, audio/video -based solutions bring challenges in
39 real implementations because of the privacy regulations. Similarly, wearable device-based methods
40 can provide customized solutions but also might lead to discomfort issues, negatively affecting their
41 feasibility. Ambient sensing (such as infrared sensors), on the other hand, relies on sensors that provide
42 only ambient information about the environment. It does not have any privacy or discomfort issues,
43 but requires careful thinking in terms of sensor placement and development of intelligent solutions that
44 can extract information from sensor data which does not provide sharp visual features to understand
45 the environment easily. Ambient sensing systems generally used for detecting human activities install
46 a large number of sensors (same or of different modality) in the environment. Each sensor brings
47 sensing noise and such noise needs to be handled before the output is fed to a sensor data fusion
48 module, a decision-making system or a machine learning model.

49 Smart spaces are usually shared by multiple people. In order to automate the facilities, i.e.,
50 heating, ventilation, air conditioning (*HVAC*), it is important to know how many people is there, at
51 which location and what do they do [2,3]. When smart offices are considered, this information is also
52 important to address security issues and an efficient meeting room occupancy management. Real-time
53 human activity detection and prediction can be used to effectively allocate resources to increase user
54 comfort in conference rooms in offices [4] as well as study-rooms in households [5]. Success of such
55 automation units can also be greatly improved with robotics systems [6].

56 On the one hand, existing solutions for occupancy prediction often require higher resolution
57 sensors that are expensive and raise privacy issues of the people who use the environment (see
58 background section for more details). On the other hand, solutions that make use of lower resolution
59 sensors have not been widely tested and their performances are mostly illustrated within controlled
60 environments where there is not sun exposure difference during the day, heat sources from other
61 objects or heat prints left from people who used the chairs and desks for a long time. Therefore, a
62 deeper analysis of the effects of this noise is necessary in order to deploy accurate solutions in real
63 environments. We believe that low-cost and low-resolution heat sensors would be helpful to create
64 easily-accessible solutions for many smart offices while avoiding privacy concerns of the people who
65 use them (it is impossible to identify the users in the environment in these low resolution images).
66 However, one of their major challenges is the high sensitivity to other heat sources; this must be
67 considered in order to provide robust algorithms which can adapt to the changing conditions of the
68 environment. Thus, in this paper, we explore how to use low-cost and low-resolution heat sensors
69 looking for solutions that are robust to noise artifacts. We present two approaches, one computer
70 vision-based and the other one, machine learning-based. We evaluate and compare their performance
71 with data recorded in a real office environment, and we discuss their advantages and disadvantages,
72 as well as their particularities regarding different heat artifacts.

73 In particular, this paper provides the following contributions:

- 74 1. We propose two different workflows (one based on computer vision and one based on machine
75 learning) for predicting the number of people in the environment.
- 76 2. We evaluate our novel workflows and provide an exhaustive analysis of their performances on a real
77 office environment where several meetings happen while the temperature and the sun illumination
78 from the windows change during the day.
- 79 3. We explain the relation of the algorithm parameters to the installation position of the sensor in the
80 office environment.
- 81 4. We use explainable AI methods in order to investigate which algorithm parameters and image
82 properties provide useful information to the classifications.
- 83 5. Finally, we focus on understanding the heat artifacts in recordings which are acquired from an

84 environment which is heavily exposed to the sunlight and used by many people in long meetings. We
85 discuss the different effects of the environmental heat artifacts (like sunlight) and the heat prints of the
86 people who sat on a specific location for a long time. We discuss the capabilities of our workflows to
87 deal with such noise artifacts and we offer compensation methods to increase accuracy of the results.

88 2. Background

89 The human activity detection problem is solved in different ways in the literature. Activity
90 detection has usually been performed using audio/video surveillance because multimedia data
91 provides very accurate representations of human activities [7]. Another method to obtain activity
92 detection is using wearable devices [8]. This method has gained a lot of attention due to that wearable
93 devices have become widely-available and popular. Nevertheless, limitations of wearable device
94 -based applications are obvious. First of all, people might forget or does not cooperate with the wearing
95 sensors. Secondly, new people visiting the environment cannot be tracked when they do not have
96 sensors.

97 Due to the high prices and the privacy issues raised by surveillance cameras, a lot of companies
98 and researchers turned their focus on using low-cost and low-resolution sensors for keeping the
99 prices low and keeping people's privacy in the scene. Passive infrared (PIR) and heat sensors became
100 interesting for such applications and researchers have focused on developing algorithms which can
101 extract information even when the data cannot obviously tell all important visual properties of the
102 scene.

103 Wahl et al. [9] used PIR sensors to recognize activities, and to keep track of how many people
104 where in a room. Murao et al. [10] used PIR sensors which are distributed in a house, in order to track
105 the activation patterns of the sensors. They used these patterns to recognize activities, and to keep
106 track of how many people where there. Even though PIR sensors are very low-cost, available to many
107 researchers and they keep the privacy of the people involved, when they are used in a constrained
108 area like a meeting room, the sensors need to be placed on all areas or objects of interest, as presented
109 in [11]. Such an application requires many sensors even in one room, at all locations where they could
110 interfere with the activity being performed. Multiple devices also means that installation, maintenance,
111 sensor fusion etc. require more effort, even if the sensors are "tape and forget", as argued in [11].
112 Besides, even though one PIR sensor is much cheaper than one heat sensor, when so many of them are
113 necessary in one room, the whole application might cost even more than a heat sensor alternative.

114 Heat sensors (infra-red sensors/cameras) provide heat images that can be conveniently used
115 to tracking people, as they only can visualize heat reflections. Heat sensors can be used to detect
116 and track people [12,13]. While higher resolution sensors provide more chances to algorithms to
117 provide robust solutions, the prices of the heat sensors increase exponentially with respect to their
118 increasing resolutions. Therefore, in order to keep the application low-cost, it is important to explore
119 the possibilities of developing algorithms that can make some predictions relying on information
120 extracted from images with very low resolution.

121 Some researchers looked for opportunities of using extremely low-resolution heat sensors for
122 understanding human activity indoors. Jeong et al. [14] showed that an adaptive thresholding
123 method could help to detect people using low-resolution heat sensors. Singh et al. [15] used
124 adaptive thresholding and the binary results for understanding whether people are on the floor,
125 in a standing or sitting position. Next, they extended their work towards a multiple sensor application
126 [16]. Troost [17] compared different classifiers which are trained to predict the number of people in
127 low-resolution heat sensor images. Gonzalez et al. [18] used a single sensor and trained a classifier
128 to differentiate 21 different activities in the environment. The experiments gave successful results to
129 show that it is possible to rely on such low-resolution image information to understand the usage of
130 the environment. Johansson and Sandberg [19] looked for opportunities of training neural networks,
131 specifically CNNs (Convolutional Neural Network) and LSTMs (Long Short-Term Memory), in order
132 to have a mathematical model which can make predictions about the number of people visible in a

133 low-resolution heat sensor. As we see in the literature related to the usage of very low-resolution heat
134 sensors, the experiments are restricted to data sets which are acquired in controlled environments
135 (such as places that are not exposed to changing sunshine conditions from large windows – which are
136 common in office spaces). Robustness in changing environmental conditions and generalization of
137 the different algorithms tested have not been discussed either and, moreover, the research on thermal
138 noise and compensation methods is still quite limited. Thus, in this study, we focus on these aspects
139 hoping to further understand how to solve them.

140 3. Aim and objectives

141 Given the challenges of the studies described in the previous section, the aim of this work is
142 to explore low-cost and privacy preserving solutions for occupancy prediction that are robust and
143 accurate and take into account the noise artifacts of the environment. After exploring possible solutions
144 that fulfilled these criteria, we suggested two alternative possible workflows based on two different
145 methods. One method heavily relies on the use of computer vision algorithms while the second
146 method relies on feature engineering (finding good/representative features in data) and solving the
147 occupancy prediction problem through machine learning. Considering these two different workflows
148 that we present in this work, we herein tackle the following three research questions:

- 149 • *Can we rely on computer vision or machine learning based methods in order to provide robust occupancy*
150 *prediction solutions when we use a low-cost and low-resolution sensor?*
- 151 • *What is the best occupancy prediction accuracy that we can achieve when computer vision based or*
152 *machine learning based methods are used?*
- 153 • *What are the sources of the noise artifacts and what are the possible noise compensation methods to*
154 *overcome errors caused by them?*

155 4. Scenario and data

156 The low-cost low-resolution heat sensor used in this study¹ [20] as well as the environment used to
157 collect the data are presented in Figs. 1 and 2. The sensor description is provided by the manufacturer
158 at [21]. Table 1 shows the heat recording data set which we have used for testing our algorithms. The
159 data set was collected in three different dates using the same sensor which was located at the office
160 ceiling, as shown in Fig. 2. The figure also depicts the labels for the chair ID's which we have indicated
161 whether there is a person or not in the data set description part of the Table 1. In the table, the blue
162 highlighted rows correspond to the sensor recordings which are captured when the room is empty.
163 Later, we will use these recordings for noise analysis and noise compensation. For the performance
164 analysis of the workflow 1 and workflow 2, we have used the Day 1 and Day 2 data set. We have used
165 the 24 hours recording of the Day 3 data for the assessment of the explainability methods since the
166 recording includes significant environment temperature changes.

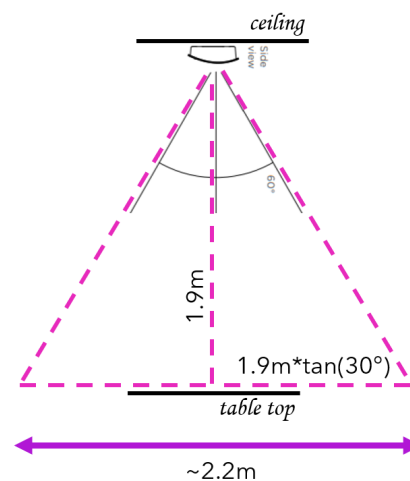


Figure 1. The low-cost and low-resolution heat sensor used in this study [20].

¹ <https://www.rolergo.com/sensors>



(a)



(b)

Figure 2. (a) The meeting room where the test data streams were collected. The sensor was placed at the ceiling, 1.9 m above the table. The seat numbers correspond to the person presence numbers in Table 1. (b) Field of view calculation for the meeting room setup. Table top line corresponds to the black line at the table edge with 90 cm measurement in (a).

167 5. Methods

168 In this section, we introduce two different workflows in order to determine the number of people
 169 in each frame (image) of the heat sensor recordings. The first method uses traditional computer vision
 170 algorithms (aka computer vision based occupancy prediction), while the second one is a machine
 171 learning-based solution. The machine learning based approach creates a feature vector for each frame,
 172 and after that, a supervised classification algorithm learns how to fit an optimal model in order to
 173 be able to classify feature vectors for identifying the number of people in the scene (we refer to this
 174 solution as feature classification based occupancy prediction). In the reminder of this section, we focus
 175 on the theory of the modules which construct our workflows, and we provide detailed analysis with
 176 the different data sets in the *Experimental Results* section.

Data label	Description	Total people	Total frames
$h_1(x, y)$	Day1 before meeting	0	94
$h_2(x, y)$	Day1 after meeting	0	45
$h_3(x, y)$	Day1 present at 1	1	24
$h_4(x, y)$	Day1 present at 1 2	2	30
$h_5(x, y)$	Day1 present at 1 2 3	3	27
$h_6(x, y)$	Day1 present at 1 2 3 4	4	51
$h_7(x, y)$	Day1 present at 2 3 4	3	29
$h_8(x, y)$	Day1 present at 3 4	2	36
$h_9(x, y)$	Day1 present at 4	1	35
$h_{10}(x, y)$	Day2 before meeting	0	94
$h_{11}(x, y)$	Day2 present at 1 2	2	56
$h_{12}(x, y)$	Day2 present at 2 3	2	47
$h_{13}(x, y)$	Day2 present at 3	1	28
$h_{14}(x, y)$	Day2 present at 3 4	2	31
$h_{15}(x, y)$	Day3 24 hours	max 2	661

Table 1. Presence sensor recordings used for testing our algorithms.

177 5.1. Computer vision based occupancy prediction

178 Fig. 3 presents the workflow of the computer vision based occupancy prediction approach. This
 179 solution requires a baseline, i.e., a recording when the office is empty. Each module of the workflow is
 180 described in detail hereafter.

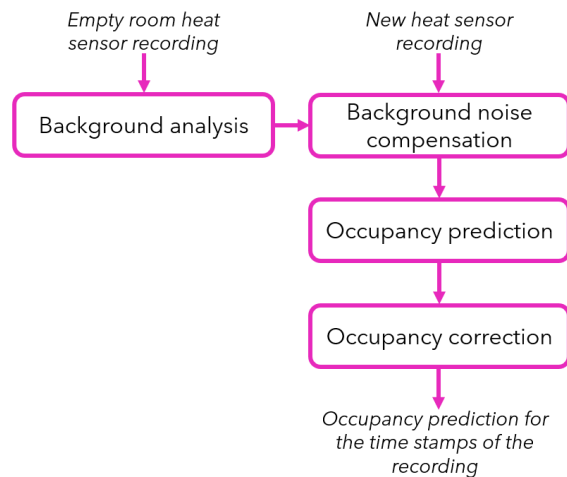


Figure 3. Workflow of the computer vision based occupancy prediction method.

181 5.1.1. Background analysis

182 We assume that we can improve the quality of each frame by removing the noise effects coming
 183 from other heated objects in the environment, such as computer like devices or other objects exposed
 184 to sunlight coming from windows. We assume that we can use a short recording of the empty room
 185 before any meeting for compensation of such heat artifacts. To do so, we calculate the mean and the
 186 standard deviation of each pixel in an empty room recording with our background analysis algorithm
 187 1. Thus, the background analysis module provides the mean ($m(x, y)$) and standard deviation ($s(x, y)$)
 188 of each pixel value through the recording of the empty room. Later on, when a new heat sensor
 189 recording is captured, these two matrices are used for background noise compensation.

190 The blue highlighted rows in Table 1 indicate the recordings which are considered for doing the
 191 background analysis. Fig. 4 shows the empty room mean and standard deviation based on those three
 192 recordings ($h_1(x, y)$, $h_2(x, y)$ and $h_{10}(x, y)$).

Algorithm 1: Background analysis algorithm

$h_i(x, y)$: Input frames

$m(x, y)$ and $s(x, y)$: Mean and standard deviation

Data: Empty room recording where i is a constant and n represents each frame

1 **Function** backgroundAnalysis($h_i^n(x, y)$):

2 $m(x, y) = \text{mean}(h_i^n(x, y))$

3 $s(x, y) = \text{std}(h_i^n(x, y))$

4 **return** $m(x, y)$ and $s(x, y)$

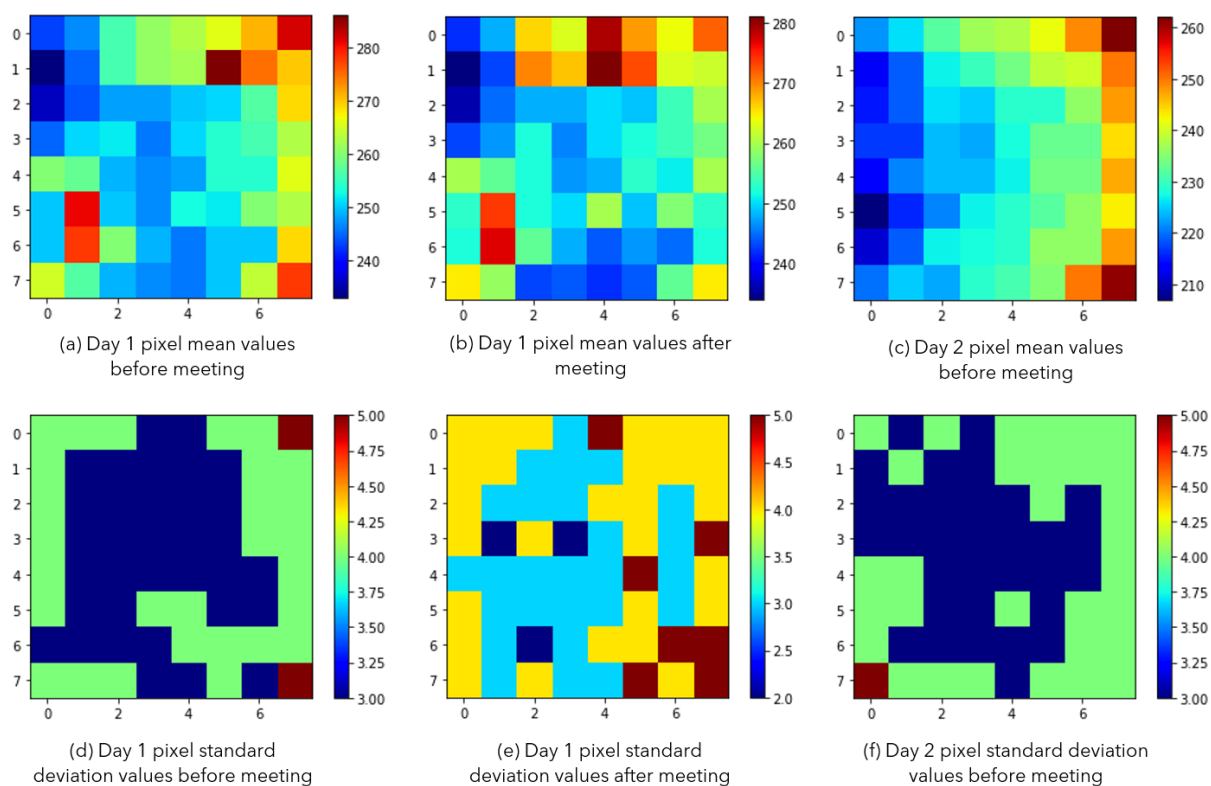


Figure 4. (a) and (b) show the pixel mean values ($m(x, y)$) for the empty room recording in Day 1 data ($h_1(x, y)$ and $h_2(x, y)$) before and after meeting, (c) shows the pixel mean values for the empty room recording in Day 2 data ($h_{10}(x, y)$) before meeting, (d) and (e) show the pixel standard deviation values ($s(x, y)$) for Day 1 data ($h_1(x, y)$ and $h_2(x, y)$) before and after meeting, (f) shows the pixel standard deviation values for ($h_{10}(x, y)$).

193 As seen in Fig. 4, there are two empty office recordings in Day 1 and one empty room recording
 194 in Day 2. The recordings of Day 1 are taken before and after a meeting that took place in the office. The
 195 Day 2 recording is taken only before the meeting. When we compare the *before meeting* recordings of
 196 two different days (a and c), we notice that the mean values are different. We understand that, even
 197 though there are no heat prints from people yet, the environment is heated differently because of the
 198 sunlight exposure from large windows. Day 2 looks sunnier and warmer. Standard deviations of the
 199 frames for those recordings (d and f) look similar. However, even though the sunlight exposure did
 200 not change during the recordings of Day 1, before and after meeting recordings show some differences.
 201 We see a slight increase in the mean values (a and b). Besides, the standard deviations look higher for

202 the after meeting recording (d and e are compared). We believe that the difference is caused by the heat
 203 prints left on the seats and the table edges where people was located.

204 5.1.2. Background noise compensation

205 We use $s(x, y)$, calculated in the previous step, for removing the pixels that we cannot trust. For
 206 instance, if the heat fluctuation (standard deviation) of a pixel is larger than a pre-determined threshold
 207 value, we do not use that pixel in the further process (we simply change the corresponding pixel
 208 values to zero in the occupied room recordings). If all pixels of $s(x, y)$ have values lower than the
 209 threshold temperature, then $s(x, y)$ matrix has no impact to the further processing steps. In our studies,
 210 we have chosen the heat threshold as 50 (corresponding to 5 Celsius degrees), since we have noticed
 211 that a human heat print cause more than 50 standard deviations when we compared to the standard
 212 deviation of the empty office.

213 For removing the background noise, we have conducted experiments by employing the *Fine*
 214 *Grained Saliency approach* [22]. This method creates real-time saliency maps that indicate the image
 215 regions which look different than their surroundings. With this method, we expected to extract the heat
 216 resources which might indicate both people and also noisy pixels. Even though this saliency method
 217 gives very successful results on high resolution images, it did not perform well on our low-resolution
 218 data. Therefore, we believe that the noise compensation method that we proposed above is a reliable
 219 solution for this case, and, in general, when low resolution images are used.

220 We provide an example heat image frame before and after the background noise compensation in
 221 Fig. 5. There is one person in this data, however the original recording had very high heat levels on
 222 the right top and bottom pixels. The difference clearly shows that the background noise compensation
 223 algorithm can eliminate the noisy pixels and highlight the person in the scene.

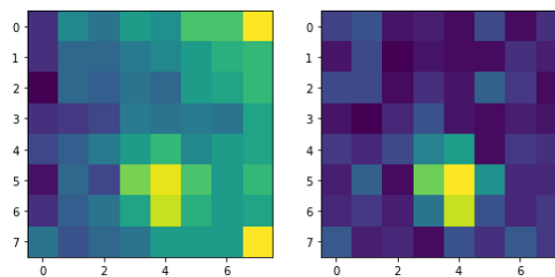


Figure 5. Left; the first frame of the $h_{13}(x, y)$ recording as an example of raw heat image having one person in the scene. Right; the same frame after applying the background noise removal technique.

224 5.1.3. Occupancy prediction

225 After the background noise compensation is applied, we apply adaptive filtering and create a
 226 binary image from each frame [23]. After obtaining the binary image, we apply a bounding box around
 227 each binary segment.

228 The field of view of the sensor is 60 degrees in both vertical and horizontal directions [20]. In Fig.
 229 2 (b), we approximate the coverage area of each heat sensor frame as a side view. Considering the
 230 height of the sensor, we expect $2.2 \times 2.2m^2$ coverage area in the table top level. This means that, when
 231 we divide the area into 8×8 , each pixel shows approx. an area of $0.27 \times 0.27m^2$. Assuming that one
 232 person covers between $0.5 \times 0.5m^2$ to $0.75 \times 0.75m^2$ (top view), we expect one person to cover from 2
 233 to 3 pixels width in the image when a bounding box is located on the detected region.

234 Based on this assumption, when a bounding box width or height is larger than 3 pixels, we count
 235 the number of people by dividing the ($width \times height$) to 3×3 and rounding the result to make it an
 236 integer value. In this way, we count the number of people in each frame. This predicted value can be
 237 presented real-time. However, if a correction is needed (because of any heat noise fluctuation during

238 the recording), then the following correction module offers filtering and produces a post-processed
239 result.

240 5.1.4. Occupancy correction

241 After the real-time computations of the predictions are done, we post-process the results for
242 correcting possible miscalculated frames. After we extracted the number of people in each frame of
243 the whole recording, we filter the predicted values using a 5 frame size median filter. This means that,
244 if the predicted number of people in the i th frame is N_i , the filter considers $[N_{i-2}, N_{i-1}, N_i, N_{i+1}, N_{i+2}]$
245 for $i \geq 2$ for applying the median filter. Of course, this parameter should be chosen carefully, since it
246 will affect the detection performance. If the frame size is small, e.g. 3, the filtering method would not
247 be able to remove the noisy results which appear more than 3 times in sequential frames. If the frame
248 size is large, then there are more chances to remove the noisy results which appear in sequential frames;
249 however, the larger filter size can also remove true detection results when the number of people really
250 changes in some frames for a very short time period. Therefore, this trade-off should be considered
251 when tuning this parameter, depending on the expected noise and the expected human movement in
252 the recordings.

253 5.2. Feature classification based occupancy prediction

254 The workflow of the second approach for occupancy prediction is presented in Fig. 6. In contrast
255 to the previous approach, we do not need a baseline image that represents an empty room, but we
256 need labelled heat sensor recordings in order to train our classifier. With a reasonable good amount of
257 labelled sensor recordings as example, we could train the classifier only once to use it new sensor data
258 later on. With "labelled heat sensor recordings", we mean that we need to know how many people
259 are seen in the scene for each frame. It is not necessary to label the pixels of the frames in order to
260 show where these people are located, since we are not concerned with the locations of the people in
261 the scene. Nevertheless, we would like to extract representative features and train our classifier so it
262 can identify the number of people in new frames. In the following sections, we describe each module
263 of the workflow in detail.

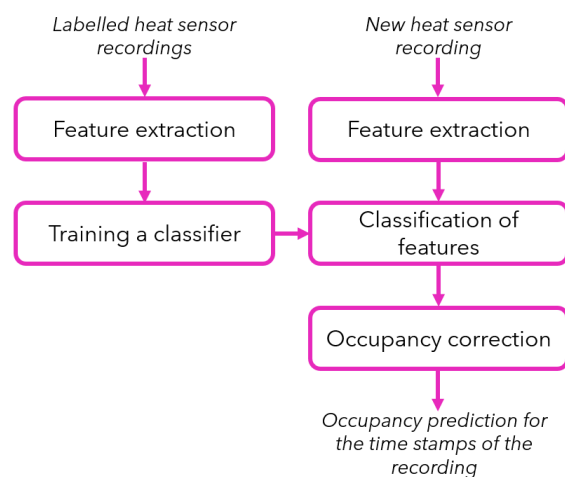


Figure 6. Workflow of the feature classification based occupancy prediction method.

264 5.2.1. Feature extraction

265 For each i th frame of a $h^i(x, y)$ heat recording, a feature vector is constructed as $f_i =$
266 $[\sigma_i, \mu_i, \min(h^i(x, y)), \max(h^i(x, y))]$. Here, σ_i and μ_i correspond to the standard deviation and mean
267 values of all pixel within the i th frame called $h^i(x, y)$. $\min(h^i(x, y))$ and $\max(h^i(x, y))$ correspond to
268 the smallest and the largest pixel values within the i th frame. Naming the four components of the f_i

269 feature vector as $[f_0, f_1, f_2, f_3]$, we have plotted the $[f_1, f_2, f_3]$ feature values for the Day 2 recordings in
 270 Fig. 7. Since we can only visualize 3 feature components at a time without applying feature reduction,
 271 we chose to visualize all but f_0 ; compared to the scales of the other feature components, f_0 varies
 272 in a very small scale which means that it is hard to visualize how the differences contribute to the
 273 differentiate classes.

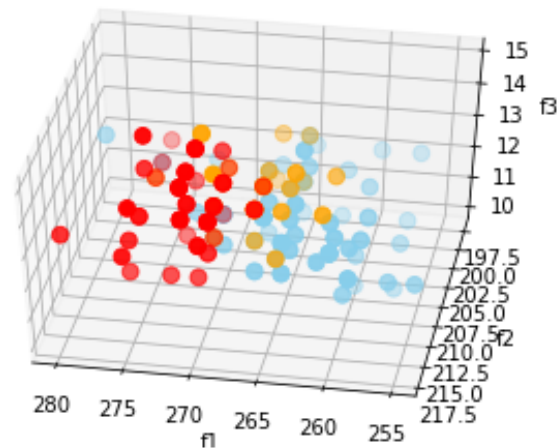


Figure 7. Training features extracted from heat sensor images of the office space when it is in three different states. Blue data points: features of the empty office recordings, Orange data points: features of the office recordings when it is occupied by one person, Red data points: features of the office recordings when it is occupied by two people.

274 Three components of the Day 2 recording features in Fig. 7, show that the feature space could be
 275 learned by a classifier in order to separate different classes showing different occupancy levels of the
 276 office.

277 5.2.2. Training a classifier

278 In order to classify f_i feature vectors, we use CatBoost classifier. CatBoost is a recently
 279 open-sourced machine learning algorithm [24]. It is able to work with diverse data types to help
 280 solving a wide range of problems that data scientists face today. “Boost” comes from gradient boosting
 281 machine learning algorithm as this library is based on a gradient boosting library. Gradient boosting is
 282 a powerful machine learning algorithm that is widely applied to multiple types of business challenges
 283 like fraud detection, recommendation systems, forecasting, etc. It can return very good results with
 284 relatively little data, unlike deep learning models that need to learn from massive amounts of data.
 285 Moreover, CatBoost works well with multiple categories of data, such as audio, text, images and
 286 historical data.

287 CatBoost is especially powerful in two ways:

- 288 1. It yields state of the art results without extensive data training typically required by other machine
 289 learning methods, and
- 290 2. It provides powerful out of the box support for the more descriptive data formats that are associated
 291 with many data science problems.

292 We use the CatBoost library [25] and trained a classifier which learns how to distinguish the feature
 293 vectors when they are labelled with the number of people in the room. As seen in the workflow from
 294 Fig. 6, the training is performed only once and the trained classifier is used to classify feature vectors
 295 when a new heat recording is processed.

296 5.2.3. Classification of features

297 When a new heat recording is captured, for each frame f_i a feature vector is extracted and the
 298 trained classifier is used to identify in which class the feature vector falls. The classification result
 299 indicates the number of people in the room for each frame. Since the CatBoost classifier performs at an
 300 excellent computational speed, even for classifications of large feature vectors, the classifier can be
 301 used in real-time applications.

302 5.2.4. Occupancy correction

303 As seen previously, the occupancy correction module can be used as a post-processing step in
 304 order to eliminate the noisy computations in frames. Occupancy correction is done with the same
 305 median filtering method introduced in the previous 5.1.4 section within the first workflow.

306 Hereafter, we introduce the results obtained after applying the two workflows previously
 307 described.

308 6. Experimental Results

309 In this section, we present the performances results of the two suggested workflows for
 310 occupancy prediction, discussing different use cases and their advantages and disadvantages. We use
 311 explainability methods in order to analyze the feature classification method of the second workflow in
 312 depth.

313 6.1. Analysis of the computer vision based method

314 We start with the performance analysis of the first workflow. Table 2 shows the performance of
 315 the computer vision based workflow for each heat recording used for testing. Here, TD stands for
 316 ‘True Detection’ which corresponds to the percentage of people who are detected correctly in an overall
 317 recording; FP stands for ‘False Positives’. We notice that the TD rate is 100% and false detection rates
 318 are almost 0% in most of the Day 2 recordings. That is probably because of the low environmental
 319 noise artifacts (less outside heat and sun rays) during this day. In Day 2 recordings, only $h_{14}(x, y)$ is
 320 processed with a lower performance. When we visualize the detection results for this data, we see that
 321 a human heat print (because of a person who changed the seat) causes a false detection, see Fig. 8(f).

Data label	Total people	Total frames	TD (%)	FP (%)	FN (%)
$h_3(x, y)$	1	24	100	100	0
$h_4(x, y)$	2	30	100	86.60	0
$h_5(x, y)$	3	27	85.19	37.03	14.81
$h_6(x, y)$	4	51	94.11	0	5.89
$h_7(x, y)$	3	29	97.50	0	2.50
$h_8(x, y)$	2	36	80.55	2.77	19.45
$h_9(x, y)$	1	35	100	80	0
$h_{11}(x, y)$	2	56	100	0	0
$h_{12}(x, y)$	2	47	100	0	0
$h_{13}(x, y)$	1	28	100	0	0
$h_{14}(x, y)$	2	31	83.8	12	3.2

Table 2. Performance of the computer vision based method on each recording which includes at least one person in the scene.

322 6.2. Analysis of the feature classification based method

323 The CatBoost classifier has been trained on the 70% randomly chosen frames of the Day 2 data set,
 324 the remainder 30% of the frames were used for testing. We obtained 97.64% classification performance
 325 (TD) with those frames. Since Day 2 data was captured with less sun exposure (as it was reported

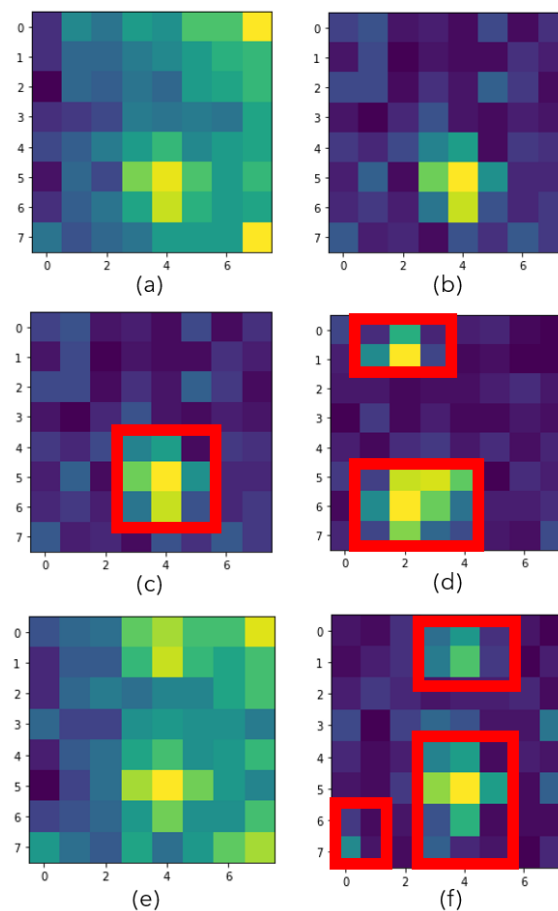


Figure 8. Analysis of the computer vision based method (workflow 1). (a) A raw image frame from $h_{13}(x, y)$ recording having one person in the scene. (b) Frame given in (a), after background noise compensation. (c) Occupancy detection result for the frame given in (a). (d) Occupancy prediction result of a frame from the $h_{12}(x, y)$ recording which has two people in the scene. (e) A raw frame from the $h_{14}(x, y)$ recording which again has two people in the scene but at different seats. (f) Occupancy prediction result of the frame given in (e) which, unfortunately, has a false positive due to the heated seat where a person was sitting earlier.

326 by the data collecting scientists), we have chosen Day 2 data to start and see the performance of our
 327 classifier on the data that we expect to find less noise. After seeing the classifier performed good, we
 328 have applied the same experiment on the Day 1 data. We re-trained the classifier (from scratch) on the
 329 the 70% randomly chosen frames of the Day 1 data set. We used the remainder 30% of the frames for
 330 testing. We achieved 95.48% performance. This result showed us that even in the presence of high
 331 noise artifacts, the classifier can be trained and give robust results.

332 Next, we have conducted experiments by using the classifier which was trained on the Day 1
 333 data for making occupancy predictions on the Day 2 data. In this case, the we have achieved 94.70%
 334 performance on the considering the true detection percentage on the Day 1 data. When we mixed Day
 335 1 and Day 2 data for training the classifier, we achieved 96.70% true detection performance on the Day
 336 1 data.

337 Thus, experiments show a high performances of the feature based occupancy prediction method,
 338 even when it trained on a different day with different environmental conditions and used on another
 339 day again. However, if one classifier is going to be used in an environment which has significantly
 340 changing noise artifacts, the classifier will perform better when data from the different times of the day
 341 (or different days) are fused to train the classifier.

342 6.3. Analysis of the feature contributions

343 As mentioned earlier, the feature vector is constructed using four properties that we extract from
 344 each frame. However, it is possible that some of these properties make a very poor contribution to the
 345 overall classification. Therefore, we borrow methods from the recent eXplainable Artificial Intelligence
 346 (XAI) [26] field of research to investigate further the influence and effect of these proprieties. We use
 347 the well-known approach SHapley Additive exPlanations (SHAP) [27] in order to determine which
 348 properties of the frames are really effective in the classification module. The goal of SHAP is to explain
 349 the prediction of an instance x by computing the contribution of each feature to the prediction. The
 350 SHAP explanation method computes Shapley values from coalitional game theory. The feature values
 351 of a data instance act as players in a coalition; Shapley values tell us how to fairly distribute the
 352 "payout" (= the prediction) among the features.

353 Fig. 9 presents the SHAP analysis results when Day 2 feature based CatBoost classifier training
 354 is considered. We can observe that f_2 feature components (minimum values) make the biggest
 355 contribution to the classification and that the f_3 feature components (maximum values) make the
 356 second largest contribution; the least contribution comes from the f_1 feature components (mean values).
 357 From this analysis, we conclude that we could slightly speed up the second workflow process by
 358 extracting only three feature components (f_2 , f_3 and f_0) and training the classifier only with them.

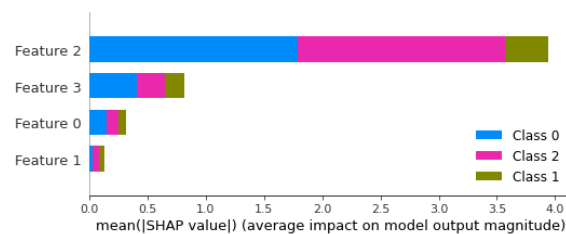


Figure 9. SHAP analysis results for the feature based classification method used in workflow 2.

359 6.4. Analysis of the noise artifacts

360 Day 1 recordings were acquired when it was very hot weather outside and the sun was shining
 361 straight through the meeting table from the large office windows (this information was provided by
 362 our industrial partner who collected the data in a real office environment). During the Day 2 data
 363 acquisition, it was rather cloudy and the meeting room was not exposed to the sun rays. We have
 364 observed the effects of the outside weather conditions in our Day 1 data set as noise artifacts. We
 365 have also achieved less performance on the Day 1 recordings than the Day 2 recordings with both two
 366 workflows. It has been obvious that the outside weather impact on the meeting room has caused noise
 367 artifacts in the data set.

368 Day 3 recordings were captured in a 24 hours time period and, thus, contain the largest outside
 369 weather condition variety. Fig. 10(a) illustrates the f_i feature components for each frame. Fig. 10(b)
 370 provides the plot of the outside temperature value in Malmö, Sweden –where the office is located–
 371 from the beginning to the end of the data acquisition process on the same date [28]. We notice a
 372 high correlation between the outside temperature and the f_1 , f_2 and f_3 feature components (mean,
 373 minimum value and maximum value, seen with the blue, green and red colors respectively). However,
 374 f_0 feature component (standard deviation of each frame seen in the magenta color plot), looks just
 375 slightly affected by the outside temperature changes. Since all four features are affected in a similar
 376 direction (even though the f_0 feature component is affected less), we believe that the second workflow
 377 can do feature classification robustly regardless of the outside temperature changes. However, the
 378 first workflow requires background correction using the mean values collected from the empty office.
 379 If the outside temperature changes a lot, this means that those values need to be re-calculated for
 380 the empty office again. When we look closely at Fig. 10(a), we notice two spikes (plotted in red) at
 381 the final frames of the recording. Tiny spikes on the same frames are also visible on the standard

382 deviation values (plotted in magenta). When we look at our RGB camera recording which we have
 383 left in the office for validation (not for computing any results, only for calculating the performances
 384 of our experiments), we notice that one person has visited the meeting room at the time when the
 385 first spike occurred. Another two people has sat on the meeting table at the time when the second
 386 spike occurred. When we used the classifier (trained on Day 2 data) on these frames, once again, we
 387 were able to predict the occupancy correctly. We have correct occupancy predictions on samples of the
 388 empty office recordings of the different time frames of the 24 hour recording as well. These results
 389 prove the robustness of the algorithm regarding the environmental noise artifacts.

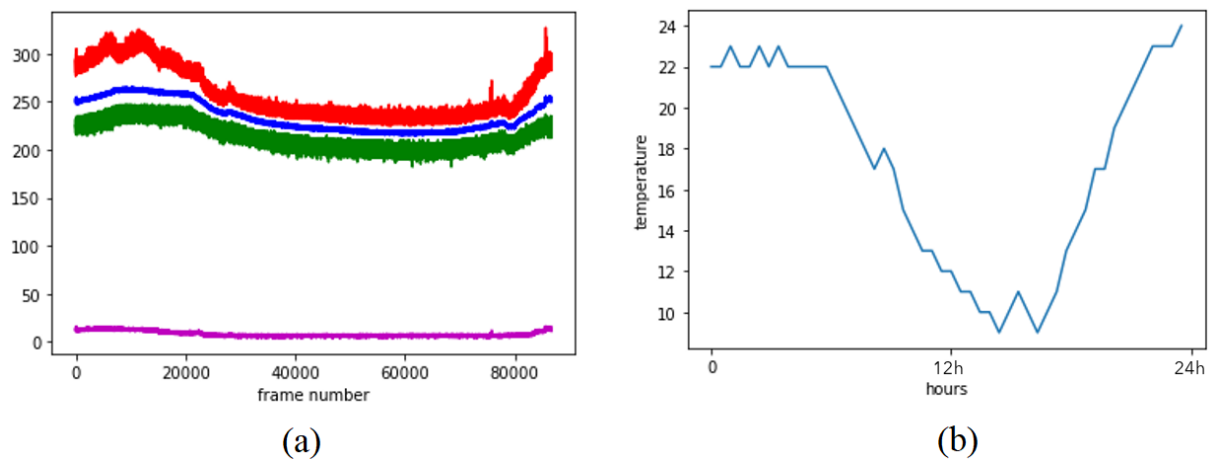


Figure 10. (a) Red; f_3 , maximum pixel value of each frame (the maximum value is around 360, which corresponds to 36 degree Celsius). Blue; f_1 mean pixel values. Green; f_2 minimum pixel values. Magenta; f_0 standard deviation of the pixel values in each frame. (b) Outside temperature in Malmö, south Sweden, from the beginning to the end of the heat sensor recording used in (a).

390 We conclude that the first workflow (computer vision -based) is more sensitive to the
 391 environmental heat noise (changing outside temperature and the hitting sun rays) than the second
 392 workflow (feature classification -based). Looking at the empty office mean and standard deviations
 393 before and after the meeting in Day 1 (see Fig. 5), we can see that the heat prints which are left from
 394 people sitting for a long time highly affect the standard deviation calculations. Therefore, the second
 395 workflow (machine learning -based) is likely to be less sensitive to the environmental heat noise, but
 396 more sensitive to the human heat print related noise artifacts.

397 6.5. Analysis of the local pixel contributions

398 For explaining the local contributions of each pixel to the classification results, we decided to
 399 use LIME (*Local Interpretable Model-agnostic Explanations*) by Ribeiro et al. [29]. The explanations
 400 given by LIME can help us to understand the trained model, and thus, transform an untrustworthy
 401 prediction into a trustworthy one. In particular, the pixels which do not make any contribution
 402 to the classification can be removed and more descriptive features can be extracted. Hence, LIME
 403 supports and complements the previous analysis carried out using SHAP, but, instead of looking at
 404 the contribution of each feature, we look at the contribution of each pixel to the classification.

405 7. Discussion

406 Herein, we will address our research questions and discuss the answers we have found with our
 407 experiments. We also highlight the lessons learned by our empirical evaluations and the application of
 408 the explainable methods.

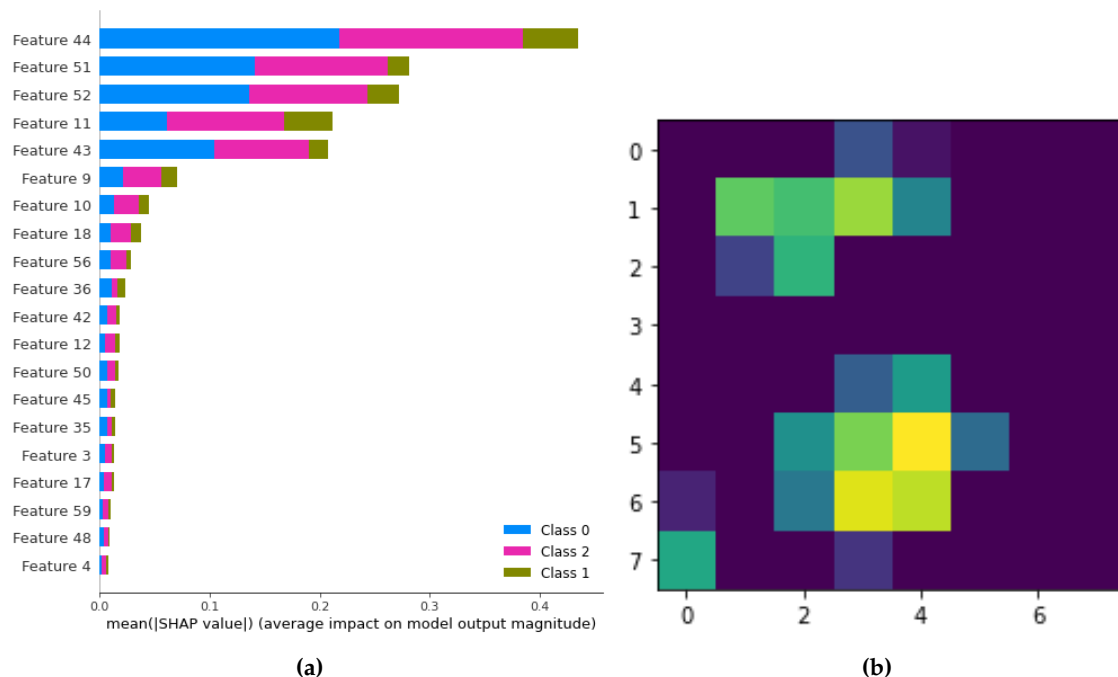


Figure 11. (a) Local contributions of pixels for performing good classifications considering heat recordings as time series for input. (b) Local contributions of each pixel are highlighted based on the explanations given in (a). Brighter pixels contribute more to the classification outcomes.

409 7.1. Can we rely on computer vision or machine learning based methods in order to provide robust occupancy
 410 prediction solutions when we use a low-cost and low-resolution sensor?

411 We answer this question by offering two different workflows in our study. We saw that, using a
 412 traditional computer vision method we can offer a robust real-time solution. However, the computer
 413 vision based method that we designed works when an empty room recording is available. When it
 414 is not possible to find such recording, our feature classification based second workflow can provide
 415 reliable results to identify the number of people within the scene.

416 7.2. What is the best occupancy prediction accuracy that we can achieve when computer vision based or machine
 417 learning based methods are used?

418 We have reached to over 80% occupancy prediction performance with the computer vision based
 419 workflow and over 90% performance with the feature classification based workflow. Choosing the
 420 right workflow for the specific use case will lead to the best performance. For instance, if it is possible
 421 to record an empty office (without human heat prints), before each meeting, we could provide reliable
 422 performances with the computer vision based method. If empty office recordings are not available,
 423 feature based algorithm are recommended.

424 7.3. What are the sources of the noise artifacts and what are the possible noise compensation methods to
 425 overcome errors caused by them?

426 We have noticed two significant noise factors which cause artifacts in our data. One is caused by
 427 the sun rays hitting directly the furniture and the objects in the office. Highly heated surfaces appear
 428 almost like a person and cause confusion to our algorithms. The second noise factor is the heat prints
 429 of people who used the room for a while (sitting at a meeting chair for half an hour, for instance).
 430 We saw that our first (computer vision based) workflow is more robust to this second kind of noise
 431 factor. However, we believe that using activity recognition methods in time series of heat recordings
 432 could increase the occupancy prediction accuracy. A time series analysis approach might also allow

433 to identify heat prints which become cooler in time (like a chair where the heat print might be lost
434 slowly).

435 7.4. Comparison of the two different workflows

436 Table 3 lists a comparison between the two proposed workflows according to the results of our
437 experiments. The table highlights the advantages and disadvantages of each workflow.

Condition	Workflow 1	Workflow 2
Dependency on an empty room recording	Good performances obtained only by having an empty room recording before meetings	It is not necessary to have an empty room recording
Dependency on a training data set	The algorithm only needs an empty room recording as a condition. Other, training data is not necessary.	The algorithm needs a training data set which includes recordings with different numbers of people in the scene.
Dependency on the environmental noise (i.e. sun exposure)	The algorithm behaves robust when similar environment is recorded when the office is empty. Otherwise, it is prone to provide false positives.	If the algorithm has such examples in the training data set, it provides reliable results.
Dependency on the human heat prints	The algorithm behaves robust, since such prints can be eliminated with the background compensation module.	The algorithm cannot easily distinguish human heat print. The algorithm is prone to provide false positives.
Dependency on other heated objects (i.e. computer, hot drinks)	The algorithm behaves robust, because of the position of our sensor (shown in Fig. 2), such objects appear too small in the images and they do not contribute as a noise factor.	Same as the Workflow 1.

Table 3. Comparison of the different occupancy prediction workflows (1 computer vision -based, 2 machine learning -based).

438 7.5. Further recommendations

439 Looking at the results provided in Fig. 4, we can make the following two suggestions in order to
440 achieve good accuracy values when using the first workflow (computer vision -based):

- 441 • For the background analysis, $m(x, y)$ and $s(x, y)$ values should be calculated when the office has
442 been empty for a while (to make sure that there are no heat prints from people)
- 443 • We recommend to re-calculate $m(x, y)$ and $s(x, y)$ when the outside heat is significantly different
444 or the sun rays are illuminating more/less powerfully than the earlier empty room recordings.

445 When the second workflow is used, we recommend to train the classifier when the noise artifacts
446 are low (no heat prints from people who left a seat and no heavy sun light exposure on the objects). If
447 the temperatures are varying significantly during the day, we recommend to train the classifier with
448 data from different times of the day.

449 8. Future work

450 Algorithm-wise, we would like to focus on trying our solutions with multiple sensor data. In
451 this case, our current efforts include: optimization of the sensor distribution in the environment,
452 synchronization of the input data, overcoming challenges coming from the overlapping views and
453 providing results based on the fused information. Secondly, we will focus on developing new
454 algorithms for identifying human activity in our low-resolution sensor recordings. We are currently
455 working on a solution based on the use of a deep neural network, specifically, Mask R-CNN [30]). We

456 have conducted some early experiments training a Mask R-CNN network which can learn identifying
457 person positions from low-resolution heat sensor images.

458 Application-wise, we are interested in bringing these smart office solutions to other fields, e.g.,
459 elderly care environments. The rapidly growing old age population in many countries has increased
460 the research that addresses challenges in ambient assisted living (AAL). Robust smart office solutions,
461 like those presented here, can be adopted in this area [31].

462 9. Conclusions

463 Herein we have proposed two new algorithm workflows for real-time occupancy prediction in
464 smart office spaces using very low-resolution heat sensor data that take into account the background
465 noise generated by the surroundings. The first workflow is based on computer vision algorithms, while
466 the second one, on feature extraction and machine learning. We have conducted experiments in order
467 to answer three major research questions related to finding reliable prediction methods, which accuracy
468 can be achieved and the identification of noise artifacts in the environment. Additionally, we have
469 used state-of-the-art explainability methods to understand how the performance of the algorithms
470 are affected by various parameters. We believe that the proposed workflows can be used in many
471 application areas related to the automation and efficient use of offices, spaces and buildings, in order to
472 improve human well-being and the efficient and sustainable use of the environment. The analysis and
473 methods employed and developed to understand the parameters and the environmental noise effects
474 on the occupancy prediction problem might help other researchers to develop robust algorithms to
475 process very low-resolution sensor data.

476 **Author Contributions:** Beril Sirmacek and Maria Riveiro have both conducted research and did authorship to
477 write this article. Beril Sirmacek has designed given workflows, prepared software solutions and conducted the
478 experiments in order to analyze the proposed workflows on the data set. Maria Riveiro has done previous work
479 for the administration of the initial project proposal and for acquisition of the project funding.

480 **Funding:** We gratefully acknowledge the grant from The Knowledge Foundation under the project MAPPE
481 (Mining Actionable Patterns from complex Physical Environments using interpretable machine learning).

482 **Acknowledgments:** Prof. Niklas Lavesson for supporting this research and our industrial partner, ROL Ergo²,
483 for their support and for collecting the data set used in this study.

484 **Conflicts of Interest:** The authors declare no conflict of interest. The funders had no role in the design of the study;
485 in the collection, analyses, or interpretation of data; in the writing of the manuscript, or in the decision to publish
486 the results.

487 Abbreviations

488 The following abbreviations are used in this manuscript:

489	AI	Artificial Intelligence
	HCI	Human Computer Interaction
	HVAC	Heating Ventilation Air Conditioning
	IoT	Internet of Things
490	LSTM	Long Short Term Memory
	ML	Machine Learning
	PIR	Passive Infrared
	SHAP	SHapley Additive exPlanations
	TD	True Detection

² <https://www.rolergo.com/>

491 **References**

- 492 1. Teixeira, T.; Dublon, G.; Savvides, A. A Survey of Human-Sensing: Methods for Detecting Presence, Count,
493 Location, Track, and Identity. *ACM Computing Surveys* **2010**, *5*, 59.
- 494 2. Agarwal, Y.; Balaji, B.; Gupta, R.; Lyles, J.; Wei, M.; Weng, T. Occupancy-driven energy management for
495 smart building automation. *BuildSys'10 - Proceedings of the 2nd ACM Workshop on Embedded Sensing Systems
496 for Energy-Efficiency in Buildings* **2010**, pp. 1–6. doi:10.1145/1878431.1878433.
- 497 3. Liang, Y.; Zhang, R.; Wang, W.; Xiao, C. Design of Energy Saving Lighting System in University
498 Classroom Based on Wireless Sensor Network. *Communications and Network* **2013**, *05*, 55–60.
499 doi:10.4236/cn.2013.51B013.
- 500 4. Offermans, S.; Kota Gopalakrishna, A.; van Essen, H.; Ozcelebi, T. Breakout 404: A smart space
501 implementation for lighting services in the office domain. *9th International Conference on Networked
502 Sensing Systems, INSS 2012 - Conference Proceedings* **2012**, pp. 1–4. doi:10.1109/INSS.2012.6240532.
- 503 5. Hsu, Y.L.; Chou, P.H.; Chang, H.C.; Lin, S.; Yang, S.C.; Su, H.Y.; Chang, C.C.; Cheng, Y.S.; Kuo, Y.C. Design
504 and Implementation of a Smart Home System Using Multisensor Data Fusion Technology. *Sensors* **2017**,
505 *17*, 1631. doi:10.3390/s17071631.
- 506 6. Piyathilaka, L.; Kodagoda, S. Human activity recognition for domestic robots. *Springer: Berlin, Germany*
507 **2015**, *26*, 395–408.
- 508 7. Sung, J.; Ponce, C.; Selman, B.; Saxena, A. Unstructured human activity detection from rgbd images. *In
509 Proceedings of the 2012 IEEE International Conference on Robotics and Automation (ICRA)* **2012**, *15*, 842–849.
- 510 8. Mukhopadhyay, S. Wearable sensors for human activity monitoring: A review. *IEEE Sens. J.* **2015**,
511 *15*, 1321–1330.
- 512 9. Wahl, F.; Milenkovic, M.; Amft, O. A Distributed PIR-based Approach for Estimating People Count in
513 Office Environments. *2012 IEEE 15th International Conference on Computational Science and Engineering* **2012**,
514 pp. 640–647.
- 515 10. Murao, K.; Terada, T.; Yano, A.; Matsukura, R. Detecting Room-to-Room Movement by Passive Infrared
516 Sensors in Home Environments. *AwareCast 2012: Workshop on Recent Advances in Behavior Prediction and
517 Pervasive Computing* **2012**.
- 518 11. Tapia, E.; Intille, S.; Larson, K. Activity Recognition in the Home Using Simple and Ubiquitous Sensors.
519 *Pervasive Comput.* **2004**, *3001*, 158–175. doi:10.1007/978-3-540-24646-6_10.
- 520 12. Olmeda, D.; de la Escalera, A.; Armingol, J.M. Detection and tracking of pedestrians in infrared images.
521 *2009 3rd International Conference on Signals, Circuits and Systems (SCS)* **2009**, pp. 1–6.
- 522 13. Doulamis, N.; Agrafiotis, P.; Athanasiou, G.; Amditis, A. Human Object Detection using Very Low
523 Resolution Thermal Cameras for Urban Search and Rescue. *Proceedings of the 10th International Conference
524 on Pervasive Technologies Related to Assistive Environments* **2017**, pp. 311–318. doi:10.1145/3056540.3076201.
- 525 14. Jeong, Y.; Yoon, K.; Joung, K. Probabilistic method to determine human subjects for low-resolution
526 thermal imaging sensor. *2014 IEEE Sensors Applications Symposium (SAS)* **2014**, pp. 97–102.
527 doi:10.1109/SAS.2014.6798925.
- 528 15. Singh, S.; Aksanli, B. Non-Intrusive Presence Detection and Position Tracking for Multiple People
529 Using Low-Resolution Thermal Sensors. *Journal of Sensor and Actuator Networks* **2019**, *8*, 40.
530 doi:10.3390/jsan8030040.
- 531 16. Shelke, S.; Aksanli, B. Static and Dynamic Activity Detection with Ambient Sensors in Smart Spaces.
532 *Sensors* **2019**, *19*, 804. doi:10.3390/s19040804.
- 533 17. Troost, M.A. Presence detection and activity recognition using low-resolution passive IR sensors. *Student
534 thesis: Master, Eindhoven University of Eindhoven, The Netherlands* **2013**.
- 535 18. Gonzalez, L.I.L.; Troost, M.; Amft, O. Using a Thermopile Matrix Sensor to Recognize Energy-related
536 Activities in Offices. *Procedia Computer Science* **2013**, *19*, 678–685. doi:10.1016/j.procs.2013.06.090.
- 537 19. Johansson, A.; Sandberg, O. A comparative study of deep-learning approaches for activity recognition
538 using sensor data in smart office environments. *Bachelor Thesis, Malmö universitet/Teknik och samhälle, Sweden*
539 **2018**.
- 540 20. Ergo, R. Presence sensor technical documentation. [https://www.rolergo.com/wp-content/uploads/
541 2019/09/PS_RIO_PRESENCE_68011023-B.pdf](https://www.rolergo.com/wp-content/uploads/2019/09/PS_RIO_PRESENCE_68011023-B.pdf), 2020.

- 542 21. PanasonicChip. Panasonic Infrared Array Sensor Grid-EYE (AMG88) Data sheet. https://cdn.sparkfun.com/assets/4/1/c/0/1/Grid-EYE_Datasheet.pdf, 2020.
- 543
- 544 22. Montabone, S.; Soto, A. Human detection using a mobile platform and novel features derived from a visual saliency mechanism. *Image and Vision Computing* **2010**, *28*, 391–402. doi:10.1016/j.imavis.2009.06.006.
- 545
- 546 23. Otsu, N. A Threshold Selection Method from Gray-Level Histograms. *IEEE Transactions on Systems, Man, and Cybernetics* **1979**, *9*, 62–66.
- 547
- 548 24. Dorogush, A.V.; Ershov, V.; Gulin, A. CatBoost: gradient boosting with categorical features support, 2018, [\[arXiv:cs.LG/1810.11363\]](https://arxiv.org/abs/1810.11363).
- 549
- 550 25. Repository. CatBoost Library. <https://github.com/catboost/catboost>, 2020.
- 551 26. Gunning, D.; Aha, D.W. DARPA's explainable artificial intelligence program. *AI Magazine* **2019**, *40*, 44–58.
- 552 27. Lundberg, S.M.; Lee, S.I. A unified approach to interpreting model predictions. *Advances in Neural Information Processing Systems* **2017**, pp. 4765—4774.
- 553
- 554 28. Time.; Website, D. Outside temperature in Malmö. <https://www.timeanddate.com/weather/sweden/malmo/historic>, 2020.
- 555
- 556 29. Ribeiro, M.; Singh, S.; Guestrin, C. "Why Should I Trust You?": Explaining the Predictions of Any Classifier. *Proceedings of the 22nd ACM SIGKDD International Conference on Knowledge Discovery and Data Mining, San Francisco, CA, USA* **2016**, pp. 1135–1144.
- 557
- 558
- 559 30. He, K.; Gkioxari, G.; Dollár, P.; Girshick, R. Mask R-CNN. *arXiv* **2017**, [\[arXiv:cs.CV/1703.06870\]](https://arxiv.org/abs/1703.06870).
- 560 31. Bourke, A.; O'Brien, J. and Lyons, G. Evaluation of a threshold-based tri-axial accelerometer fall detection algorithm. *Gait Posture* **2007**, *26*, 194—199.
- 561